Accelerating the Tempo of the Segmentation Clock by Reducing the Number of Introns in the Hes7 Gene

AUTHOR(S):

Harima, Yukiko; Takashima, Yoshiki; Ueda, Yuriko; Ohtsuka, Toshiyuki; Kageyama, Ryoichiro

CITATION:

Harima, Yukiko ...[et al]. Accelerating the Tempo of the Segmentation Clock by Reducing the Number of Introns in the Hes7 Gene. Cell Reports 2013, 3

ISSUE DATE:

2013-01-31

URL:

http://hdl.handle.net/2433/163492

Please cite this article in press as: Harima et al., Accelerating the Tempo of the Segmentation Clock by Reducing the Number of Introns in the *Hes7* Gene, Cell Reports (2013), http://dx.doi.org/10.1016/j.celrep.2012.11.012

Cell Reports
Report

Cell PRESS
Open ACCESS

Accelerating the Tempo of the Segmentation Clock by Reducing the Number of Introns in the *Hes7* Gene

Yukiko Harima,[1,3] Yoshiki Takashima,[1,5] Yuriko Ueda,[1,2] Toshiyuki Ohtsuka,[1,4] and Ryoichiro Kageyama[1,4,*]
[1]Institute for Virus Research
[2]Faculty of Medicine
Kyoto University, Kyoto 606-8507, Japan
[3]Graduate School of Biostudies, Kyoto University, Kyoto 606-8502, Japan
[4]Japan Science and Technology Agency, CREST, Shogoin-Kawahara, Sakyo-ku, Kyoto 606-8507, Japan
[5]Current address: Medical and Biological Laboratories Co., LTD, Nagoya 460-0008, Japan
*Correspondence: rkageyam@virus.kyoto-u.ac.jp
http://dx.doi.org/10.1016/j.celrep.2012.11.012

SUMMARY

Periodic somite segmentation is controlled by the cyclic gene *Hes7*, whose oscillatory expression depends upon negative feedback with a delayed timing. The mechanism that regulates the pace of segmentation remains to be determined, but mathematical modeling has predicted that negative feedback with shorter delays would give rise to dampened but more rapid oscillations. Here, we show that reducing the number of introns within the *Hes7* gene shortens the delay and results in a more rapid tempo of both *Hes7* oscillation and somite segmentation, increasing the number of somites and vertebrae in the cervical and upper thoracic region. These results suggest that the number of introns is important for the appropriate tempo of oscillatory expression and that *Hes7* is a key regulator of the pace of the segmentation clock.

INTRODUCTION

During somitogenesis, *Hes7* expression oscillates owing to delayed negative feedback in the presomitic mesoderm (PSM), and disruption of this oscillation blocks the oscillatory expression of many other genes, such as *Lfng* and *Dusp4*, leading to somite fusion (Pourquié, 2011; Oates et al., 2012; Eckalbar et al., 2012; Kageyama et al., 2012; Bessho et al., 2001; Niwa et al., 2007; Sparrow et al., 2012). This suggests that *Hes7* plays an important role in the segmentation clock, although it remains to be determined whether *Hes7* is the fundamental pacemaker or whether it acts downstream of another oscillator. The clock period can be altered by inhibition of Wnt signaling, inhibition of Notch signaling coupling, or mutations of *Nrarp* in mice or *hes6* in zebrafish (Gibb et al., 2009; Herrgen et al., 2010; Schröter and Oates, 2010; Kim et al., 2011). However, the expression of β-catenin, a Wnt signaling effector, does not cycle (Aulehla et al., 2008), and *Nrarp* and *hes6* are not essential for periodic segmentation (Wright et al., 2009; Schröter and Oates, 2010; Kim et al., 2011). Thus, oscillators that are essential for segmentation are not included in the list of genes that could affect the pace of segmentation. In addition, all mutations that have been reported to date result solely in disruption or slower tempos of the segmentation clock (Oates et al., 2012; Kageyama et al., 2012; Bessho et al., 2001; Schröter and Oates, 2010; Kim et al., 2011), and such defects are also observed under other conditions, such as lower temperatures, that slow or inhibit embryogenesis in general (Jiang et al., 2000).

Mathematical modeling suggests that negative feedback with appropriate transcriptional/translational delays, which include the time required for transcription, splicing, translation, and transport of messenger RNA (mRNA) and protein products, underlies the oscillatory expression of the segmentation clock genes (Lewis, 2003; Monk, 2003; Jensen et al., 2003; Hirata et al., 2004; Zeiser et al., 2008). The sum of such delays regulates the stability and period of the oscillation, and shorter delays would both accelerate the tempo of the oscillation and dampen or abolish it (Lewis, 2003; Monk, 2003; Jensen et al., 2003). If Hes7 is the fundamental pacemaker, manipulations that increase the frequency of Hes7 oscillation should lead to a faster tempo (i.e., a shorter period) of somite segmentation. One way to shorten the delays and accelerate Hes7 oscillation is to delete the introns, because transcription and splicing of intron sequences increase the time necessary for mRNA production. The *Hes7* gene has three introns, and deletion of all three introns reduces the delay by 19 min and completely abolishes oscillatory expression, leading to steady Hes7 expression and fusion of all somites (Takashima et al., 2011). Mathematical modeling suggests that such a short delay would abolish the oscillatory expression, and that a more moderate delay would give rise to more rapid but dampened oscillations (Takashima et al., 2011). We hypothesized that deletion of one or two introns from the *Hes7* gene would lead to such a moderate delay, leading to shorter periodicity of somite segmentation, and proceeded to test that possibility.

RESULTS AND DISCUSSION

Increasing the Number of Cervical and Upper Thoracic Vertebrae by Reducing the Number of Introns in the *Hes7* Gene

Mathematical modeling suggests that negative feedback with an appropriate delayed timing is essential for sustained oscillatory

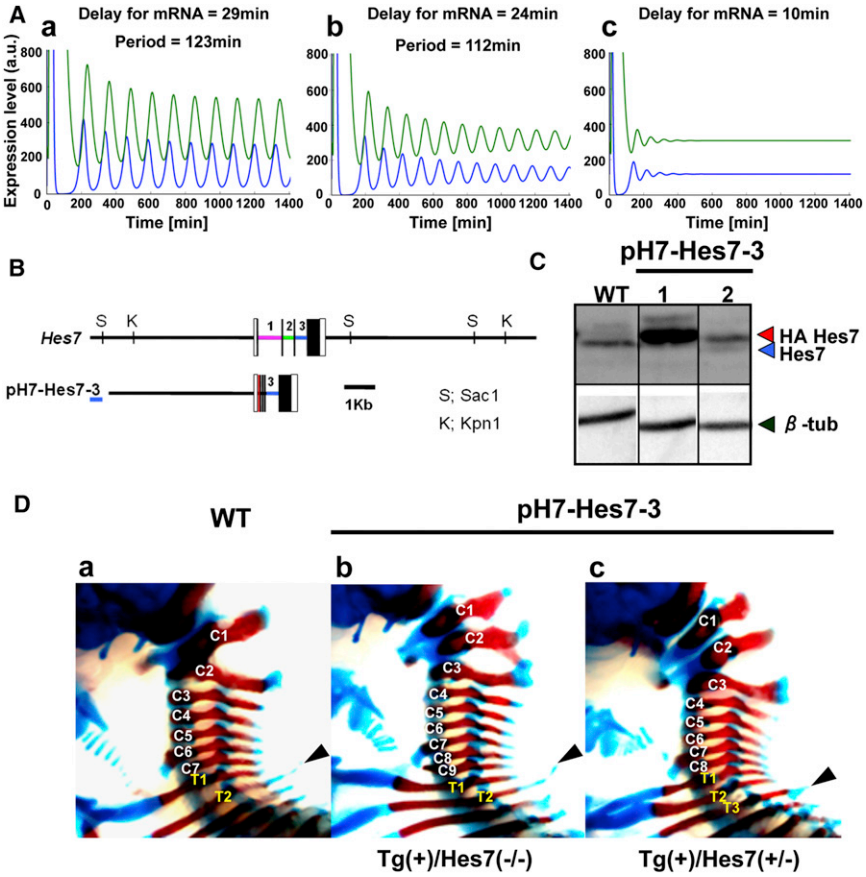

Figure 1. Increasing the Segment Number by Reducing the Number of *Hes7* Gene Introns

(A) Mathematical simulation of *Hes7* mRNA (blue) and Hes7 protein (green). The transcriptional delay (T_m) was set at 29 min for the WT (a), 24 min for a transgene containing only the third intron (b), and 10 min for a transgene lacking all introns (c).

(B) Schematic structure of the *Hes7* transgene pH7-Hes7-3.

(C) Western blot analysis of Hes7 in the PSM of WT mice and lines 1 and 2 of pH7-Hes7-3 mice. Hes7 protein expressed from the transgene is larger in size than the endogenous one because of the HA tag. Note that the endogenous Hes7 expression was suppressed in both lines of pH7-Hes7-3 mice. β-tubulin is a loading control.

(D) Bones and cartilage of the neck region of WT (a) and pH7-Hes7-3 line 1 neonates (b and c). In WT neonates, there are seven cervical vertebrae and the T2 vertebra has a longer spinous process (arrowhead). The number of vertebrae in the cervical and upper thoracic region increases in pH7-Hes7-3 mice.

See also Figures S1, S2, S3, and S4.

expression, and that reduction of the delay by 19 min would abolish the oscillatory expression (Figure 1Ac). However, a more moderate delay (for example, 5 min shorter than the wild-type [WT]) would give rise to more rapid but dampened oscillations (Figure 1Ab, 8.9% shorter period than the WT shown in Figure 1Aa). We previously showed that deletion of all three introns within the *Hes7* gene reduces the delay by 19 min and completely abolishes oscillatory expression (Takashima et al., 2011). Furthermore, we found that introduction of a *Hes7* transgene lacking introns (pH7-Hes7-0; Figure S1) into WT mice caused severe segmentation defects in a dominant fashion even though two alleles of the WT *Hes7* gene were present (Takashima et al., 2011). By contrast, introduction of the *Hes7* transgene containing the three introns, which rescued the segmentation defects in *Hes7* null mice, did not cause any defects in the WT background (pH7-Hes7-123; Figures S1, S2B, and S2C; Takashima et al., 2011). Taking advantage of this feature, we generated F0 transgenic mice carrying *Hes7* transgenes lacking either one or two introns into the WT background and examined their vertebral segmentation. *Hes7* transgenes containing two introns caused some minor segmentation defects, but most regions appeared largely normal (Figures S1 and S2D–S2F: first and second introns, pH7-Hes7-12, n = 2; first and third introns, pH7-Hes7-13, n = 2; second and third introns, pH7-Hes7-23, n = 2), suggesting that the segmentation proceeds almost normally when any two introns are present. However, introduction of *Hes7* transgenes carrying a single intron showed more severe segmentation defects (Figures S1 and S2G–S2I: first intron alone, pH7-Hes7-1, n = 7; second intron, pH7-Hes7-2, n = 2; third intron, pH7-Hes7-3, n = 4). Mice carrying a *Hes7* transgene containing either the first or third intron alone exhibited better segmentation than those carrying a transgene containing the second intron alone (Figures S2G–S2I). Interestingly, mice carrying a transgene containing the first or third intron alone had eight or nine cervical vertebrae (Figures S2G' and S2I'), whereas the WT and pH7-Hes7-123 mice had seven (Figures S2A'–S2C'). We performed subsequent experiments using the transgene containing the third intron alone (pH7-Hes7-3) because this transgene seemed to give rise to slightly better segmentations in the upper thoracic region.

We established two independent lines carrying pH7-Hes7-3 (Figure 1B) and measured Hes7 protein expression in the PSM. Line 1 expressed a high level of Hes7 protein in the PSM, whereas the level of expression by line 2 was similar to that of the WT endogenous level (Figure 1C). All line 1 mice (n = 11) exhibited eight or nine cervical vertebrae irrespective of the *Hes7* background (+/+, +/−, or −/−), and line 2 (n = 4) exhibited seven (Figures 1Db, 1Dc, and S3). Furthermore, although the second thoracic (T2) vertebra in WT mice has a longer spinous process, this feature was instead associated with the T3 vertebra in some of the line 1 mice and all of the line 2 mice (Figures 1Dc, S3C, and S3D). These results indicate that one or two additional vertebrae formed in the cervical and upper thoracic region of the mutant compared with the control mice. When two additional vertebrae formed in line 1 of pH7-Hes7-3 mice, duplication of the first cervical vertebra (C1) and extra formation of C9 or T3 seemed

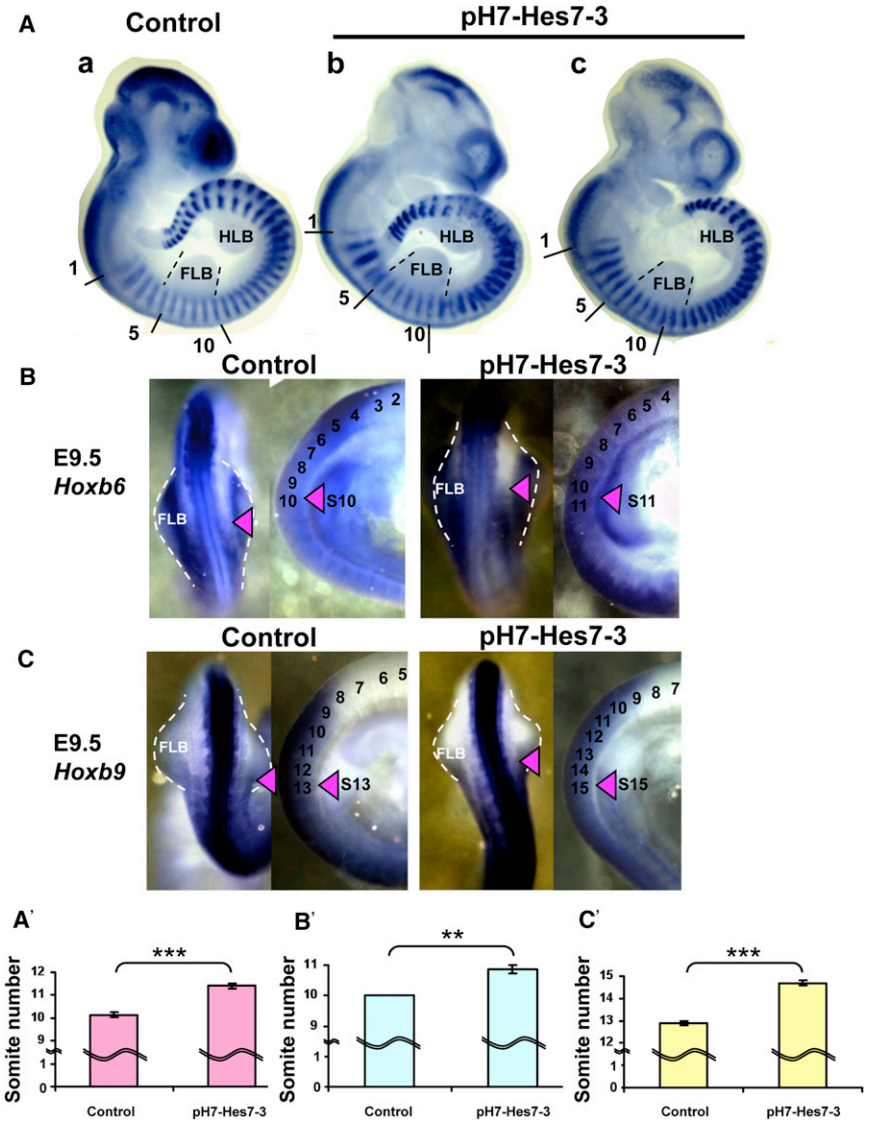

Figure 2. Increase in the Number of Somites in pH7-Hes7-3 Embryos

(A and A') Whole-mount in situ hybridization of *Uncx4.1*. The number of *Uncx4.1*-expressing somites that were present anterior to the posterior border of the forelimb and SEM were quantified in control (a, control, n = 14) and pH7-Hes7-3 line 1 mice (b and c, n = 27). Somites were normally segmented in the most caudal region of these pH7-Hes7-3 embryos, but these embryos were in the *Hes7*(+/+) or *Hes7*(+/−) background, suggesting that the WT *Hes7* may compensate in the caudal region. FLB, forelimb bud; HLB, hindlimb bud.

(B and C) Whole-mount in situ hybridization of *Hoxb6* and *Hoxb9*. The back view shows the anterior border of *Hoxb6* and *Hoxb9* expression in somites (arrowheads). The side view shows the somites. In the side view, the anterior borders of *Hoxb6* and *Hoxb9* expression in somites are hidden by strong expression in the neural tube.

(B' and C') The anterior border of *Hoxb6* (B') and *Hoxb9* (C') expression and SEM were quantified in control (n = 7 for both probes) and pH7-Hes7-3 mice (n = 7 for both probes). **p < 0.01, ***p < 0.001, t test.

to occur (Figures 1Db and 1Dc). Before cervical somites form, four pairs of occipital somites form. Furthermore, it has been reported that *Her*/*Hes* oscillation starts before the somite segmentation takes place in the chick (two cycles before somite formation) and zebrafish (five cycles before somite formation; Jouve et al., 2000; Riedel-Kruse et al., 2007). Thus, although it is unknown how many pulses of *Hes7* oscillation occur before somite formation in mouse embryos, it is possible that at least six pulses of *Hes7* oscillation occur before the first cervical somite forms. If this is the case, every six to eight somites, one extra somite could be formed in line 1. However, the vertebrae in the more-caudal region were fused in all of the pH7-Hes7-3 mice (Figure S2I). These results suggest that the segmentation clock is set at a faster tempo during the cervical and upper thoracic segmentations but is halted during the more-caudal segmentation in mice carrying pH7-Hes7-3.

We next compared the delay in gene expression from the genes lacking all introns, containing only the third intron, and containing all three introns. We used a ubiquitinated luciferase reporter under the control of the *Hes1* promoter as previously described (Takashima et al., 2011). This analysis showed that the gene containing the third intron alone expressed the reporter protein ~5 min earlier than the control gene (containing three introns) and ~13 min later than the gene containing no intron (Figure S4), which was within the expected range of in vivo splicing kinetics (Audibert et al., 2002; Singh and Padgett, 2009). Mathematical modeling predicted that such a delay caused by a transgene containing the third intron alone would lead to faster but dampened oscillation (Figure 1Ab).

Increase of the Number and Decrease of the Size of Somites in the Anterior Region of pH7-Hes7-3 Mice

We compared the numbers of somites in pH7-Hes7-3 and control embryos at approximately embryonic day 8.5 (E8.5). At this stage, the control embryos contained 6.6 ± 0.5 somites, whereas their littermates carrying pH7-Hes7-3 had 7.4 ± 1.3 somites, indicating that the latter contained on average ~0.8 more somites than the control at this stage. However, the somite number varied between embryos even in WT mice (commonly differing by three or four somites; Tam, 1981), and thus it was difficult to determine whether the observed difference was due to normal variability or a faster tempo of the segmentation clock. We therefore counted the number of somites that formed in the anterior region at E10.5 by using the forelimb as a landmark. In situ hybridization of *Uncx4.1* revealed that there were

Cell PRESS
Open ACCESS

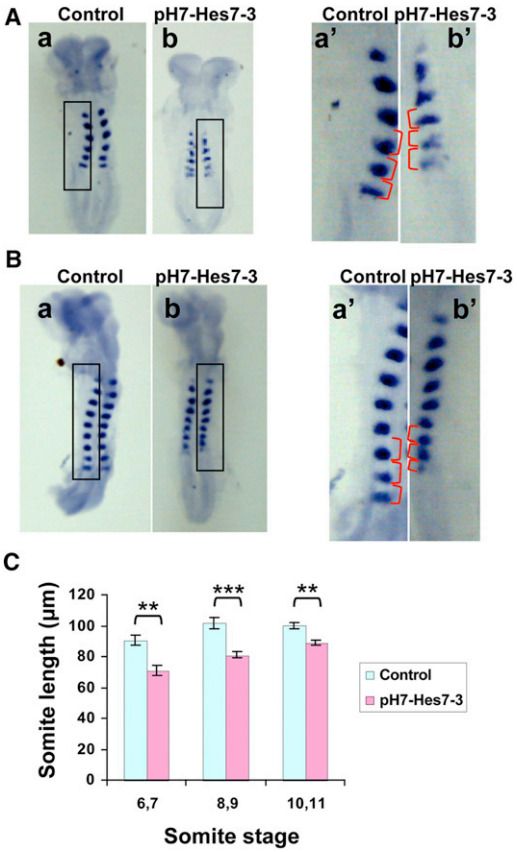

Figure 3. Shorter Somite Lengths in pH7-Hes7-3 Embryos

(A–C) The average length with SEM of the three most posterior somites was measured in control and pH7-Hes7-3 mice at 6/7-somite (A and C, n = 8 and 10 for control and pH7-Hes7-3 mice, respectively), 8/9-somite (B and C, n = 5 and 15), and 10/11-somite (C, n = 11 and 5) stages. **p < 0.01, ***p < 0.001, t test.

10.1 ± 0.1 *Uncx4.1*-expressing somites anterior to the posterior border of the forelimb in the control (Figures 2Aa and 2A'), whereas there were 11.4 ± 0.1 *Uncx4.1*-expressing somites in the same region of pH7-Hes7-3 embryos (Figures 2Ab, 2Ac, and 2A'). These results indicate that on average 1.3 additional somites form in the anterior region of the mutant. In agreement with the vertebral fusion defects in the caudal region, somites were fused caudally to the forelimb in the mutant (Figures 2Ab and 2Ac). These data suggest that the segmentation clock is set at a faster tempo but is subsequently halted during the formation of more-caudal somites.

We next examined the anterior border of *Hox* expression. The relative positions of the anterior borders of *Hoxb6* and *Hoxb9* expression to the forelimb bud were very similar between the control and pH7-Hes7-3 embryos (Figures 2B and 2C, arrowheads). However, whereas the anterior borders of *Hoxb6* and *Hoxb9* expression correspond to the 10th and 13th somites, respectively, in control mice (Alexander et al., 2009), they corresponded on average to the 10.9th and 14.7th somites, respectively, in the mutant (Figures 2B, 2B', 2C, and 2C'). These results suggest that the anterior border of *Hoxb6* and *Hoxb9* expression was shifted caudally by one or two additional somites in pH7-Hes7-3 embryos, supporting the idea of a faster tempo of the segmentation clock. This result also indicates that the link between the segmentation clock and *Hox* gene activation (Zákány et al., 2001) can be easily dissociated, as observed in zebrafish *hes6* mutation (Schröter and Oates, 2010).

If the segmentation clock were set at a greater frequency, the somite size would be smaller, in contrast to the larger somites observed when the clock cycles at a slower frequency (Schröter and Oates, 2010). Therefore, we compared the lengths of the three most recently formed somites between control and pH7-Hes7-3 embryos at the same stages. We found that they were reduced by 10%–20% in pH7-Hes7-3 embryos compared with the control at various stages (Figure 3). These data suggest that the tempo of somite segmentation is increased in mice carrying pH7-Hes7-3.

Accelerated Tempo of the Segmentation Clock of pH7-Hes7-3 Mice

To show decisively that the tempo of *Hes7* oscillation and somite segmentation is accelerated in pH7-Hes7-3 embryos, we performed time-lapse imaging of whole-embryo cultures at E8.5. We examined *Hes7* oscillations by using the *Hes7* reporter pHes7-UbLuc (Takashima et al., 2011; Niwa et al., 2011). In control embryos, *Hes7* expression oscillated with an average period of 126.6 ± 2.0 min (Figures 4A, 4C, and 4D; Movie S1). Furthermore, somite segmentation occurred with a similar periodicity (Figure 4A; Movie S1). In contrast, in pH7-Hes7-3 embryos, *Hes7* expression oscillated with an average period of 115.4 ± 1.1 min (8.8% shorter than the control), and somite segmentation also occurred with the same periodicity (Figures 4B–4D; Movie S2). These data indicate that removal of the two introns leads to a more rapid tempo of *Hes7* oscillation and somite segmentation.

It has been mathematically predicted that altering the delay in negative feedback of clock genes should alter the oscillation period. Indeed, altering the intron length of an artificial oscillator gene results in alteration of the period (Swinburne et al., 2008). However, Stauber et al. (2012) recently reported that elongation of the intron length of another oscillator gene, *Lfng*, had no effect on the segmentation period. Thus, they were not able to alter the period by changing the delays in negative feedback of the natural clock genes. This could be because such an elongation was insufficient to cause a significantly longer delay. Alternatively, *Lfng* may not be a pace-making clock gene, because its oscillation is regulated by *Hes7* (Bessho et al., 2001). Stauber et al. (2012) also attempted to elongate the intron length of the essential oscillator gene *Hes7*, but this abolished its expression, and therefore they were not able to change the period. Here, we found that reducing the number of introns in the *Hes7* gene led to a faster tempo of the segmentation clock, which suggests that *Hes7* is a pace-making clock gene for somite segmentation. Our study also shows that the number of introns is very important for the period and stability of oscillatory expression. Complete lack of introns abolishes oscillatory expression (Takashima et al., 2011), whereas removal of two introns leads to a more frequent but dampened oscillation. In

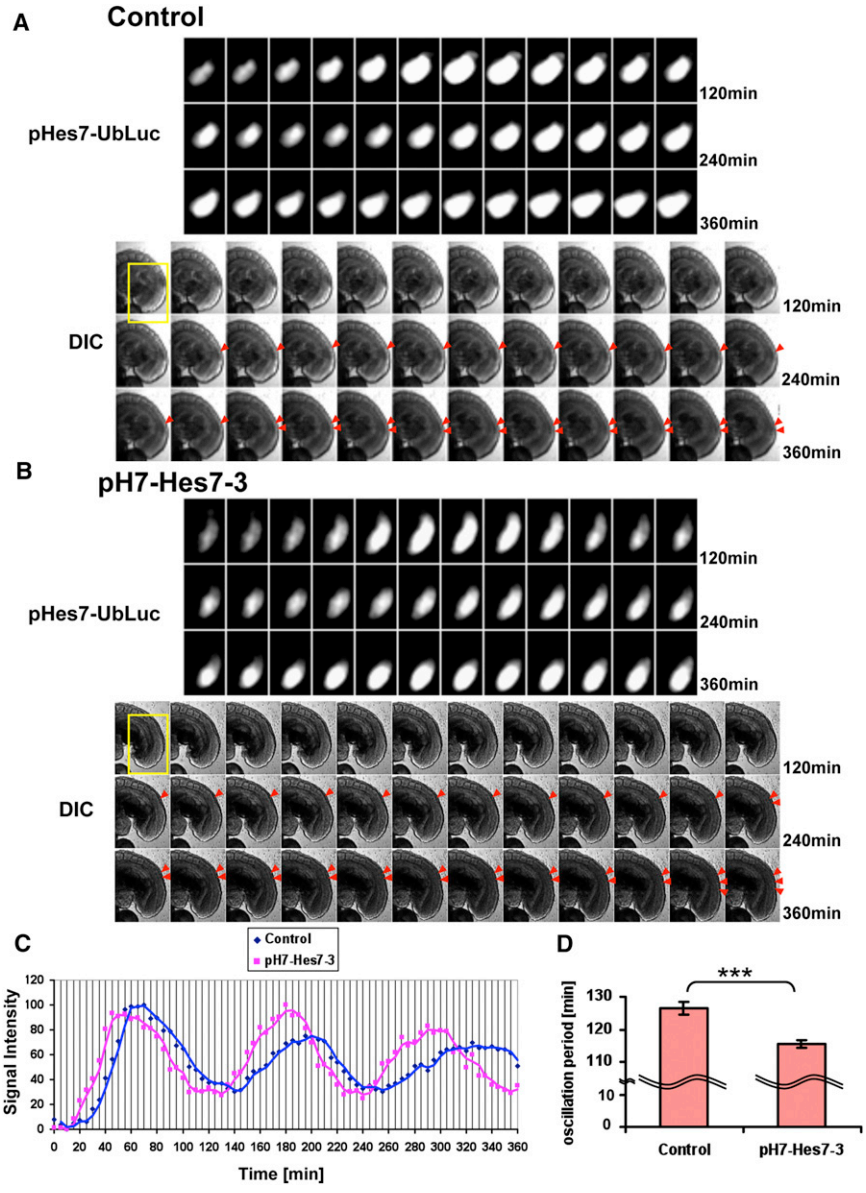

Figure 4. Accelerated Tempo of *Hes7* Oscillation and the Segmentation Clock

(A and B) Time-lapse imaging of *Hes7* oscillation and segmentation in control (A) and pH7-Hes7-3 (B) embryos at E8.5. A side view of the posterior region is shown. The yellow boxed region is enlarged for bioluminescence images. Newly formed somite boundaries are indicated by arrowheads.

(C) Quantification of the *Hes7* reporter expression.

(D) Quantification of the *Hes7* oscillation period. The average period with SEM of at least three cycles of each embryo was measured. Control, n = 14; pH7-Hes7-3, n = 20. ***p < 0.001, t test.

contrast, the presence of two introns led to mostly normal segmentation, although there were some minor defects in caudal regions. Interestingly, another mouse oscillator gene, *Hes5*, has two introns (Takebayashi et al., 1995; Dunwoodie et al., 2002). Furthermore, the essential zebrafish oscillator genes *her1* and *her7* contain three and two introns, respectively (Gajewski et al., 2003). These data suggest that at least two introns are required for oscillatory expression of the segmentation clock genes, and point to the significant role of introns in the timing of gene expression.

EXPERIMENTAL PROCEDURES

Mathematical Simulation

Hes7 oscillations were simulated with the following equations as previously described (Hirata et al., 2004):

$$\frac{dp(t)}{dt} = am(t - T_p) - bp(t)$$

$$\frac{dm(t)}{dt} = f(p(t - T_m)) - cm(t)$$

where $p(t)$ and $m(t)$ are the quantities of functional Hes7 protein and *Hes7* mRNA per cell at time t, respectively; $f(p)$ is the rate of initiation of transcription, which depends on the amount of the protein, p, present at the time of initiation; a is the rate constant for translation; and b and c are the degradation rate constants for Hes7 protein and *Hes7* mRNA, respectively, which are related to the half-lives of the molecules:

$$b = \frac{\ln 2}{\tau_p}, \quad c = \frac{\ln 2}{\tau_m}.$$

Because transcription is inhibited by a dimer of Hes7 protein, we assume

$$f(p) = \frac{k}{\left\{1 + \left(\frac{p}{p_{crit}}\right)^2\right\}}$$

where k is the number of molecules of *Hes7* mRNA synthesized per unit time in the absence of inhibition, and p_{crit} is the amount of protein that gives half-maximal inhibition. We set a = 4.5 protein molecules per mRNA molecule per min, p_{crit} = 40 molecules per cell, k = 33 mRNA molecules per cell per min, τ_m = 3 min. We assume that the Hes7 protein half-life τ_p = 20 min, T_p = 8 min, and T_m = 29 min. Under these conditions, oscillatory expression continues (Figure 1Aa). In contrast, when T_m = 10 min (19 min shorter), oscillations are abolished (Figure 1Ac). When T_m = 24 min (5 min shorter), oscillations occur at a faster tempo but soon dampen (Figure 1Ab).

Transgenic Mice

The *Hes7* transgene with three introns (pH7-Hes7-123) consisted of the genomic fragment of the *Hes7* promoter region (5,393 bp upstream fragment from the first codon), a hemagglutinin (HA) tag fragment at the amino terminus, and a genomic sequence from the second codon to 76 bp downstream of the putative polyadenylation signal. To remove one or two introns, the intron-exon regions were replaced with *Hes7* cDNA fragments. For the intronless *Hes7* transgene (pH7-Hes7-0), the whole *Hes7* coding and intron regions were replaced with *Hes7* cDNA. Transgenic mice were generated by injecting linearized constructs without any vector sequence into the pronucleus of fertilized eggs. Mice carrying the *Hes7* reporter pH7-UbLuc-In(−) were previously described (Takashima et al., 2011).

Cell PRESS
Open ACCESS

Genotyping was performed by PCR using the following primers:

WT mice: 5′-AGAAAGGGCAGGGAGAAGTGGGCGAGCCAC-3′ and 5′-GTTCTGAGAGCGAGAGGGGGTCTGGGATGG-3′

Hes7 null mice: 5′-AGAAAGGGCAGGGAGAAGTGGGCGAGCCAC-3′ and 5′-TTGGCTGCAGCCCGGGGGATCCACTAGTTC-3′

pH7-Hes7-3 mice: 5′-CGTACCAGATTACGCTATGGTC-3′, 5′-CCCAAGCCTGCTCCTTG-3′ and 5′-ACGGCGAACTCTAATATCTCCGCTTTCTC-3′

pH7-UbLuc-In(−) reporter mice: 5′-TACTGGTCTGCCTAAAGGTG-3′ and 5′-CCACCAGAAGCAATTTCGTG-3′

Western Blotting

The PSM parts of four embryos were mixed with 15 μl of lysis buffer (50 mM Tris-HCl pH 8.0, 100 mM NaCl, 5 mM $MgCl_2$, 0.5% NP-40, 1× proteinase inhibitor cocktail, 1 mM phenylmethanesulfonylfluoride, 250 U/ml Benzonase) and incubated on ice for 30 min. After addition of 1.5 μl of 10% SDS, the samples were boiled and the protein concentrations were measured. The protein solution was boiled in sample buffer and then run on 12.5% SDS-PAGE. After the protein was transferred from the gel to polyvinylidene fluoride membrane (Millipore), the membrane was immersed in buffer containing 5% skim milk, anti-Hes7 antibody (1/300; Bessho et al., 2003), and peroxidase-conjugated anti-guinea pig immunoglobulin G (IgG, 1/4,000; Chemicon) in sequence. Immunoreactive bands were visualized with ECL-plus (GE Healthcare) and LAS 3000mini (Fuji Film). The intensity of each band was calculated with Image Gauge (Fuji Film). After the antibodies were stripped, the membrane was immersed in buffer containing 5% skim milk, anti-β-tubulin IgG (Santa Cruz), and peroxidase-conjugated anti-rabbit IgG (GE Healthcare) in sequence. Immunoreactive bands were visualized with ECL (GE Healthcare).

Bone and Cartilage Staining

Bone and cartilage of neonates were stained with alizarin red and alcian blue, respectively, as described previously (Bessho et al., 2001).

Whole-Mount In Situ Hybridization

Whole-mount in situ hybridization was performed as described previously (Bessho et al., 2001). For *Hoxb6* and *Hoxb9* probes, we amplified the genomic fragments by PCR using the following primers: 5′-TACCAGACCCTGGAGCTGGAG-3′ and 5′-ACCGAAGTATTTCACGTCCGG-3′ (*Hoxb6*), and 5′-TACCAGACCCTGGAGCTGGAG-3′ and 5′-CTAGTGGATCCTCAGGGCTCC-3′ (*Hoxb9*).

Bioluminescence Imaging of the PSM

All images were recorded in 16 bit with Image-Pro Plus (Media Cybernetics) and other equipment as described previously (Masamizu et al., 2006) with the following modifications: a 10× UPlan FLN objective lens (NA 0.30) was used with 4×4 binning and exposure time of 4 min 30 s. Images were analyzed with ImageJ software.

SUPPLEMENTAL INFORMATION

Supplemental Information includes four figures and two movies and can be found with this article online at http://dx.doi.org/10.1016/j.celrep.2012.11.012.

LICENSING INFORMATION

ACKNOWLEDGMENTS

We thank H. Miyachi for help in generating the transgenic mice, and H. Shimojo, A. Isomura, and Y. Niwa for technical help and discussion. This work was supported by Grants-in-Aid from the Ministry of Education, Culture, Sports, Science and Technology of Japan.

Received: September 14, 2012
Revised: October 26, 2012
Accepted: November 15, 2012
Published: December 6, 2012

REFERENCES

Alexander, T., Nolte, C., and Krumlauf, R. (2009). *Hox* genes and segmentation of the hindbrain and axial skeleton. Annu. Rev. Cell Dev. Biol. *25*, 431–456.

Audibert, A., Weil, D., and Dautry, F. (2002). In vivo kinetics of mRNA splicing and transport in mammalian cells. Mol. Cell. Biol. *22*, 6706–6718.

Aulehla, A., Wiegraebe, W., Baubet, V., Wahl, M.B., Deng, C., Taketo, M., Lewandoski, M., and Pourquié, O. (2008). A beta-catenin gradient links the clock and wavefront systems in mouse embryo segmentation. Nat. Cell Biol. *10*, 186–193.

Bessho, Y., Sakata, R., Komatsu, S., Shiota, K., Yamada, S., and Kageyama, R. (2001). Dynamic expression and essential functions of Hes7 in somite segmentation. Genes Dev. *15*, 2642–2647.

Bessho, Y., Hirata, H., Masamizu, Y., and Kageyama, R. (2003). Periodic repression by the bHLH factor Hes7 is an essential mechanism for the somite segmentation clock. Genes Dev. *17*, 1451–1456.

Dunwoodie, S.L., Clements, M., Sparrow, D.B., Sa, X., Conlon, R.A., and Beddington, R.S.P. (2002). Axial skeletal defects caused by mutation in the spondylocostal dysplasia/pudgy gene *Dll3* are associated with disruption of the segmentation clock within the presomitic mesoderm. Development *129*, 1795–1806.

Eckalbar, W.L., Fisher, R.E., Rawls, A., and Kusumi, K. (2012). Scoliosis and segmentation defects of the vertebrae. WIREs Dev. Biol. *1*, 401–423.

Gajewski, M., Sieger, D., Alt, B., Leve, C., Hans, S., Wolff, C., Rohr, K.B., and Tautz, D. (2003). Anterior and posterior waves of cyclic her1 gene expression are differentially regulated in the presomitic mesoderm of zebrafish. Development *130*, 4269–4278.

Gibb, S., Zagorska, A., Melton, K., Tenin, G., Vacca, I., Trainor, P., Maroto, M., and Dale, J.K. (2009). Interfering with Wnt signalling alters the periodicity of the segmentation clock. Dev. Biol. *330*, 21–31.

Herrgen, L., Ares, S., Morelli, L.G., Schröter, C., Jülicher, F., and Oates, A.C. (2010). Intercellular coupling regulates the period of the segmentation clock. Curr. Biol. *20*, 1244–1253.

Hirata, H., Bessho, Y., Kokubu, H., Masamizu, Y., Yamada, S., Lewis, J., and Kageyama, R. (2004). Instability of Hes7 protein is crucial for the somite segmentation clock. Nat. Genet. *36*, 750–754.

Jensen, M.H., Sneppen, K., and Tiana, G. (2003). Sustained oscillations and time delays in gene expression of protein Hes1. FEBS Lett. *541*, 176–177.

Jiang, Y.J., Aerne, B.L., Smithers, L., Haddon, C., Ish-Horowicz, D., and Lewis, J. (2000). Notch signalling and the synchronization of the somite segmentation clock. Nature *408*, 475–479.

Jouve, C., Palmeirim, I., Henrique, D., Beckers, J., Gossler, A., Ish-Horowicz, D., and Pourquié, O. (2000). Notch signalling is required for cyclic expression of the hairy-like gene *HES1* in the presomitic mesoderm. Development *127*, 1421–1429.

Kageyama, R., Niwa, Y., Isomura, A., González, A., and Harima, Y. (2012). Oscillatory gene expression and somitogenesis. WIREs Dev. Biol. *1*, 629–641.

Kim, W., Matsui, T., Yamao, M., Ishibashi, M., Tamada, K., Takumi, T., Kohno, K., Oba, S., Ishii, S., Sakumura, Y., and Bessho, Y. (2011). The period of the somite segmentation clock is sensitive to Notch activity. Mol. Biol. Cell *22*, 3541–3549.

Lewis, J. (2003). Autoinhibition with transcriptional delay: a simple mechanism for the zebrafish somitogenesis oscillator. Curr. Biol. *13*, 1398–1408.

Masamizu, Y., Ohtsuka, T., Takashima, Y., Nagahara, H., Takenaka, Y., Yoshikawa, K., Okamura, H., and Kageyama, R. (2006). Real-time imaging of the somite segmentation clock: revelation of unstable oscillators in the individual presomitic mesoderm cells. Proc. Natl. Acad. Sci. USA *103*, 1313–1318.

Monk, N.A.M. (2003). Oscillatory expression of Hes1, p53, and NF-kappaB driven by transcriptional time delays. Curr. Biol. *13*, 1409–1413.

Oates, A.C., Morelli, L.G., and Ares, S. (2012). Patterning embryos with oscillations: structure, function and dynamics of the vertebrate segmentation clock. Development *139*, 625–639.

Pourquié, O. (2011). Vertebrate segmentation: from cyclic gene networks to scoliosis. Cell *145*, 650–663.

Niwa, Y., Masamizu, Y., Liu, T., Nakayama, R., Deng, C.X., and Kageyama, R. (2007). The initiation and propagation of Hes7 oscillation are cooperatively regulated by Fgf and notch signaling in the somite segmentation clock. Dev. Cell *13*, 298–304.

Niwa, Y., Shimojo, H., Isomura, A., González, A., Miyachi, H., and Kageyama, R. (2011). Different types of oscillations in Notch and Fgf signaling regulate the spatiotemporal periodicity of somitogenesis. Genes Dev. *25*, 1115–1120.

Riedel-Kruse, I.H., Müller, C., and Oates, A.C. (2007). Synchrony dynamics during initiation, failure, and rescue of the segmentation clock. Science *317*, 1911–1915.

Schröter, C., and Oates, A.C. (2010). Segment number and axial identity in a segmentation clock period mutant. Curr. Biol. *20*, 1254–1258.

Singh, J., and Padgett, R.A. (2009). Rates of *in situ* transcription and splicing in large human genes. Nat. Struct. Mol. Biol. *16*, 1128–1133.

Sparrow, D.B., Chapman, G., Smith, A.J., Mattar, M.Z., Major, J.A., O'Reilly, V.C., Saga, Y., Zackai, E.H., Dormans, J.P., Alman, B.A., et al. (2012). A mechanism for gene-environment interaction in the etiology of congenital scoliosis. Cell *149*, 295–306.

Stauber, M., Laclef, C., Vezzaro, A., Page, M.E., and Ish-Horowicz, D. (2012). Modifying transcript lengths of cycling mouse segmentation genes. Mech. Dev. *129*, 61–72.

Swinburne, I.A., Miguez, D.G., Landgraf, D., and Silver, P.A. (2008). Intron length increases oscillatory periods of gene expression in animal cells. Genes Dev. *22*, 2342–2346.

Takashima, Y., Ohtsuka, T., González, A., Miyachi, H., and Kageyama, R. (2011). Intronic delay is essential for oscillatory expression in the segmentation clock. Proc. Natl. Acad. Sci. USA *108*, 3300–3305.

Takebayashi, K., Akazawa, C., Nakanishi, S., and Kageyama, R. (1995). Structure and promoter analysis of the gene encoding the mouse helix-loop-helix factor HES-5. Identification of the neural precursor cell-specific promoter element. J. Biol. Chem. *270*, 1342–1349.

Tam, P.P.L. (1981). The control of somitogenesis in mouse embryos. J. Embryol. Exp. Morphol. Suppl. *65*, 103–128.

Wright, D., Ferjentsik, Z., Chong, S.W., Qiu, X., Jiang, Y.J., Malapert, P., Pourquié, O., Van Hateren, N., Wilson, S.A., Franco, C., et al. (2009). Cyclic Nrarp mRNA expression is regulated by the somitic oscillator but Nrarp protein levels do not oscillate. Dev. Dyn. *238*, 3043–3055.

Zákány, J., Kmita, M., Alarcon, P., de la Pompa, J.L., and Duboule, D. (2001). Localized and transient transcription of *Hox* genes suggests a link between patterning and the segmentation clock. Cell *106*, 207–217.

Zeiser, S., Rivera, O., Kuttler, C., Hense, B., Lasser, R., and Winkler, G. (2008). Oscillations of Hes7 caused by negative autoregulation and ubiquitination. Comput. Biol. Chem. *32*, 47–51.